We are IntechOpen, the world's leading publisher of Open Access books
Built by scientists, for scientists

6,900
Open access books available

185,000
International authors and editors

200M
Downloads

154
Countries delivered to

Our authors are among the

TOP 1%
most cited scientists

12.2%
Contributors from top 500 universities

BOOK CITATION INDEX
CLARIVATE ANALYTICS
INDEXED

WEB OF SCIENCE™

Selection of our books indexed in the Book Citation Index
in Web of Science™ Core Collection (BKCI)

Interested in publishing with us?
Contact book.department@intechopen.com

Numbers displayed above are based on latest data collected.
For more information visit www.intechopen.com

Toward Human Like Walking – Walking Mechanism of 3D Passive Dynamic Motion with Lateral Rolling – Advances in Human-Robot Interaction

Tomoo Takeguchi, Minako Ohashi and Jaeho Kim
Osaka Sangyo University
Japan

1. Introduction

It may not be so science fiction any more that robots and human live in the same space. The robots may need to move like human and to have shape of humanoid in order to share the living space. Some robots may be required to walk along with human for special care. This requires robot to be able to walk like human and to sense how humans walk. Human walks by maximizing walking in between passive walking and active walking in effective manner such as less energy, less time, and so on (Ishiguro & Owaki, 2005). It is important to clarify the mechanisms of passive walking. This study is the first step to decrease the gap between robots and human in motion, advance in human-robot interaction.

Most robots use actuators at each joint, and follow a certain selected trajectory in order to walk as mentioned active walking before. So, considerable power source is necessary to drive and control many actuators in joints.

On the other hand, human swings a leg, leans its body forward, and uses potential energy in order to walk as if human tries to save energy to walk. Walking down the slope is one of the easiest conditions to walk (Osuka, 2002). The application of these human walking to the robots is called passive dynamic walking. A possibility to reproduce passive dynamic walking experimentally is introduced by McGeer (McGeer, 1990). Giving a simply structured walker proper initial conditions, the walker walks down the slope by inertial and gravitational force without any artificial energy externally.

Goswami et al. carry out extensive simulation analysis, and show stability of walking and several other phenomena (Goswami et al., 1998; Goswami et al., 1998). In addition, Osuka et al. reproduce passive dynamic walking and the phenomena experimentally by using Quartet (walker)(Osuka et al., 1999; Osuka et al., 2000).

However, the both studies constrain the yaw and rolling motion in order to simplify the analyses. Also, these analyses are made for legs without knees, so that extra care was necessary to make experimental analyses harder because the swing legs hit the slope at the position that it passes the supporting leg.

In this study, the analyses were made three-dimensional walking with rolling motion. The 3D modeling, and simulation analysis were performed in order to search better walking

condition and structural parameters. Then, the 3D passive dynamic walker was fabricated in order to analyze the passive dynamic walking experimentally.

2. Modelingof 3D passive walker

A compass gait biped model for walking is a model which constrains the motion into a two dimensional plane. The walker for this model has to have four or eight legs to cut off the rolling motion for experimental analyses. In addition, there is foot-scuffing problem at the time when a swing leg is passing the side of support leg.

So, 3D passive walker model is used to solve the problems stated above, and to investigate the stableness of the walker. The modeling and simulation of this study was inspired by Tedrake et al. (Tedrake, 2004; Tedrake et al., 2004).

2.1 3D Model of passive walker

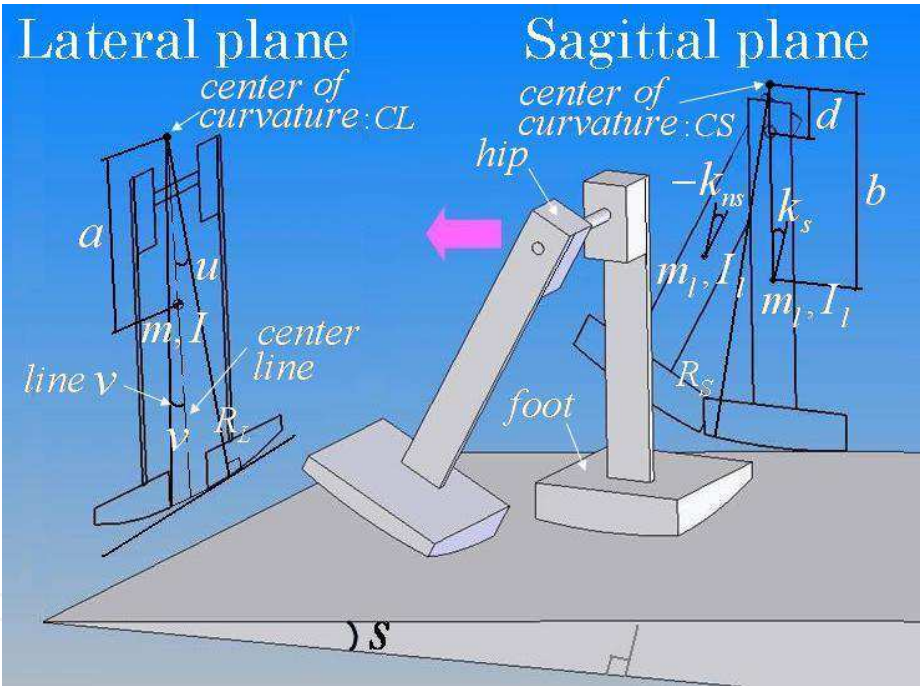The 3D model of passive walker is shown in Fig. 1. Each parameters used in this model is shown in Table1 and 2.

Fig. 1. 3D Model of Passive Walker

Symbol	Lateral Plane	Quantity
M	Mass	2.5 kg
I	Inertia	533 kgcm²
R_L	Radius of foot curve	50 cm
A	Distance between CL and center of gravity	29 cm
U	Angle of rolling	
V	Angle between center line and line v	0.038 rad

Table 1. Parameters for Model in Lateral Plane

Symbol	Sagittal Plane	Quantity
m_l	Mass of a leg	1.25 kg
l_I	Inertia of a leg	47.4 kgcm²
R_s	Radius of foot curve	38 cm
B	Distance CS and center of leg	17 cm
D	Distance between the center of curvature and hip	4.7 cm
k_s	Angle of swing leg	
k_{ns}	Angle of support leg	
S	Angle of slope	0.035 rad

Table 2. Parameters for model in sagittal plane

This model is a 3-D passive walker with two legs connected at hip with simple link structure. Legs do not have knees. Foot with concaved surface allows the rolling motion, so that walking is expanded 3D space. Especially, the rolling motion in lateral plane solves the scuffing problem at the moment when swing leg is passing through supporting leg. In sagittal plane, support leg can be seen as an inverted pendulum, and swing can be seen as simple pendulum for the motion of bipedaling walker.

The assumption that the yaw motion was small enough to ignore was made for simplifying the numerical analysis, and analysis was carried in a way the space is dividing into lateral and sagittal plane.

2.2 Equation of motion for lateral plane

The equation of motion for lateral plane is given. It is assumed that the foot of support leg is on contact and not slipping with surface of slope until becoming swing leg.

$$H(u)\ddot{u} + C(u,\dot{u})\dot{u} + G(u) = 0 \tag{1}$$

$H(u)$ is a matrix for inertial force, $C(u,\dot{u})$ is a matrix for centrifugal force, and $G(u)$ is a vector for gravitational force in (1). For this equation, the component would change according to the angle of rolling, u.

When only supporting leg is on contact on slope ($|u| > v$), the each component is shown in (2).

$$H(u) = I + ma^2 + mR_L^2 - 2mR_L a \cos u$$

$$C(u,\dot{u}) = mR_L a\dot{u} \sin u$$

$$G(u) = mga \sin u \tag{2}$$

When changing the supporting leg ($|u| \le v$), the each component is shown in (3).

$$H(u) = I + ma^2 + mR_L^2 - 2mR_L a \cos(u - w)$$

$$C(u,\dot{u}) = 0$$

$$G(u) = mg(a \sin u - R_L \sin w) \tag{3}$$

Under condition of u>0, w is defined as w=u-v, and under condition of u<0, w is defined as w=u+v in (3).

When the angle of rolling is zero (u=0), the swing leg collides with slope. This collision is assumed to be inelastic collision. The equation of collision can be shown as (4).

$$\dot{u}^+ = \dot{u}^- \cos[2\tan^{-1}\left(\frac{R_L \sin v}{R_L \cos v - a}\right)] \tag{4}$$

Superscripts - and + means before and after collision accordingly in (4).

2.3 Equation of motion for sagittal plane

The equation of motion for sagittal plane is shown as (5).

$$H(q)\ddot{q} + C(q,\dot{q})\dot{q} + G(q) = 0 \tag{5}$$

q is a vector for angle of support and swing leg, H(q) is a 2 by 2 matrix for inertial force, $C(q,\dot{q})$ is a 2 by 2 matrix for centrifugal force in (5). G(q) is a vector for gravitational force in (5). The components of (5) can be expressed in (6).

H(u) is a matrix for inertial force, $C(u,\dot{u})$ is a matrix for centrifugal force, and G(u) is a vector for gravitational force in (1). For this equation, the component would change according to the angle of rolling, u.

When only supporting leg is on contact on slope ($|u|$ >v), the each component is shown in (2).

$$H_{11} = I_1 + m_1 b^2 + m_1 d^2 + m_1 R_s^2 - 2m_1 R_s(b+d)\cos(k_s - s)$$

$$H_{12} = H_{21} = m_1(b-d)\{d\cos(k_s - k_{ns}) - R_s \cos(k_{ns} - s)\}$$

$$H_{22} = I_1 + m_1(b-d)^2$$

$$C_{11} = m_1 R_s(b+d)\sin(k_s - s)\dot{k}_s + \frac{1}{2}m_1 d(b-d)\sin(k_s - k_{ns})\dot{k}_{ns}$$

$$C_{12} = m_1(b-d)\{d\sin(k_s - k_{ns})(\dot{k}_{ns} - \frac{1}{2}\dot{k}_s) + R_s \sin(k_{ns} - s)\dot{k}_{ns}\}$$

$$C_{21} = m_1(b-d)\{d\sin(k_s - k_{ns})(\dot{k}_{ns} - \frac{1}{2}\dot{k}_s) - \frac{1}{2}R_s \sin(k_{ns} - s)\dot{k}_{ns}\}$$

$$C_{12} = \frac{1}{2}m_1(b-d)\{d\sin(k_s - s) + R_s \sin(k_{ns} - s)\}\dot{k}_s$$

$$G_1 = m_1 g\{(b+d)\sin k_s - 2R_s \sin s\}$$

$$G_2 = m_1 g(b-d)\sin k_{ns} \tag{6}$$

The equation for collision can be shown for before and after the collision by the conservation law for angler momentum in (7)

$$Z^+(q)\dot{q}^+ = Z^-(q)\dot{q}^- \tag{7}$$

Superscripts - and + means before and after collision accordingly in (7). $Z^+(q)$ and $Z^-(q)$ are matrices for the coefficients of collision. Components in (7) are shown as (8).

$$Z_{11}^- = 2bd\cos(k_{ns} - k_s) - (b+d)R_s\cos(k_{ns} - s) - 2bR_s\cos(k_{ns} - s) + 2R_s^2 + b^2 - bd$$

$$Z_{12}^- = Z_{21}^- = (b-d)\{b - R_s\cos(k_{ns} - s)\}$$

$$Z_{22}^- = 0$$

$$Z_{11}^+ = (b-d)\{d\cos(k_s - k_{ns}) - R_s\cos(k_s - s) + (b-d)\}$$

$$Z_{12}^+ = -R_s(b-d)\cos(k_s - s) - R_s(b+2d)\cos(k_{ns} - s) + d^2 + 2R_s^2 + bR_s\cos(k_{ns} + s)$$

$$-b^2\cos(2k_{ns}) + d(b-d)\cos(k_s - k_{ns})$$

$$Z_{21}^+ = (b-d)^2$$

$$Z_{22}^+ = (b-d)\{d\cos(k_s - k_{ns}) - R_s\cos(k_s - s)\} \tag{8}$$

3. Simulation results

Structural parameters and numerical parameters are searched for stable walking motion. Since there is no effective theory for the stability analysis, the only way is to try the simulations for the conditions those can be realized for the experiments. Some comparisons are made for limit cycles in order to decide the better conditions as shown in Fig. 2 and 8. These results show that limit cycle can be changed drastically in a small difference in two

(a) $m_l = 1.4$, $I_l = 48$ (b) $m_l = 1.5$, $I_l = 49$
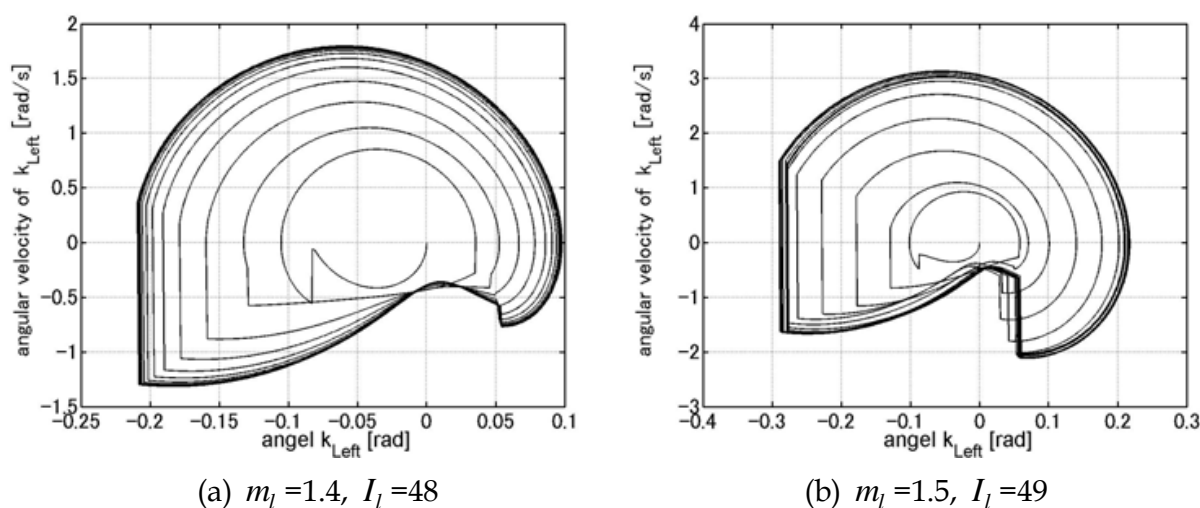
(m_l in kg, I_l in kgcm^2)

Fig. 2. Limit Cycles around Better Condition

parameters shown. Fig. 2 (a) shows limit cycle. This may be a better condition comparing with Fig. 2 (b) which does not show limit cycle. However, Fig. 2 (a) requires more cycles to converge into the limit cycle comparing with the Fig. 8. The results shown bellow are the ones of better results or better tendency from searching parameters although the method is primitive. Table 1 and 2 show parameters and initial conditions used for better walking results. In order to start walking, initial angle of rolling was applied as 0.18 rad.

3.1 Simulation results for lateral plane

The walking motion in lateral plane is shown schematically in Fig.3. A walking starts from scene 1, and follow the arrows for rolling motion. One cycle of gait is starting from the scene one and just before coming back to scene one again.
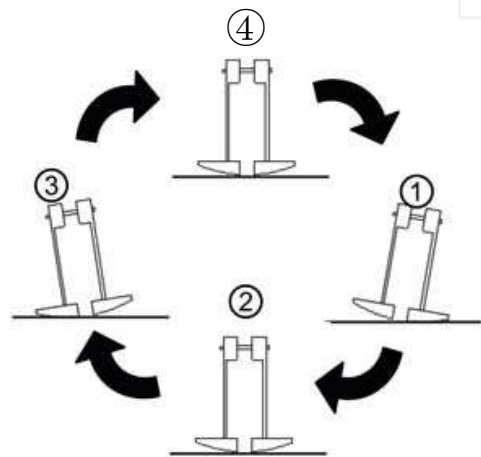
Fig. 3. Motion of Model in Lateral Plane

Fig.4 shows the change in angle of rolling with time. The amplitude of the angle attenuates gradually, and period of walking shortens slowly as time passes.
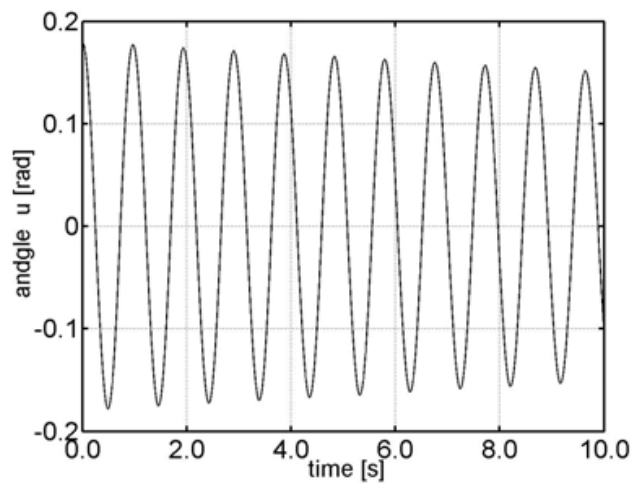

Fig. 4. Angle of Roll in Lateral Plane

Fig. 5 shows the phase plane locus for the angle of rolling for 5 seconds from the beginning of walking. The trajectory starts from the initial condition, $(u, \ddot{u}) = (0.18, 0)$, and converges into the condition, $(u, \ddot{u}) = (0, 0)$. The reason for this phenomenon is the collision at scene 2 and 4 in Fig. 3, and the angular velocity decreases slightly.
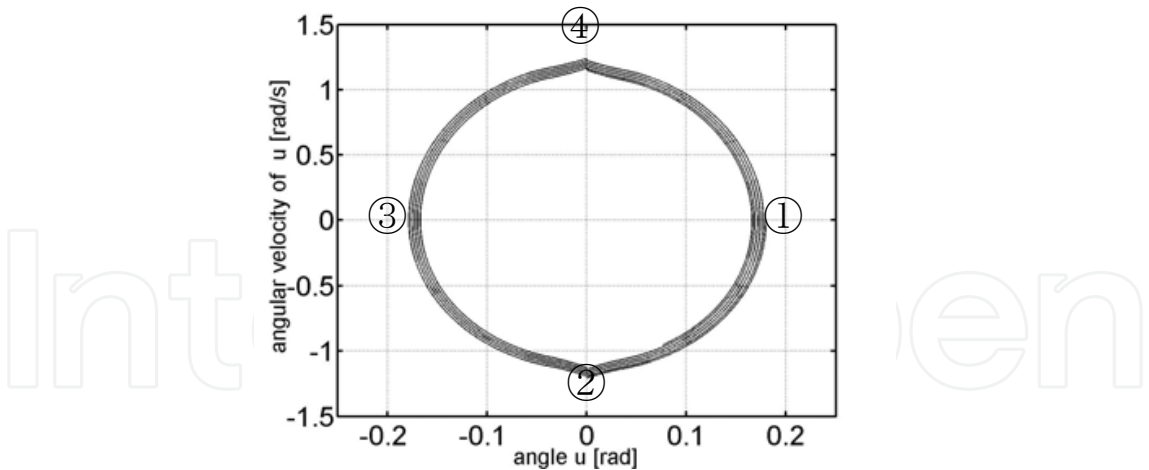
Fig. 5. Phase Plane Locus in Lateral Plane

3.2 Simulation results for sagittal plane

The walking motion in sagittal plane is shown schematically in Fig. 6. A walking starts from scene 1, and follows the arrows as the walker walks down the slope. The motion from scene 1 to just before scene one is defined as one cycle of gait.
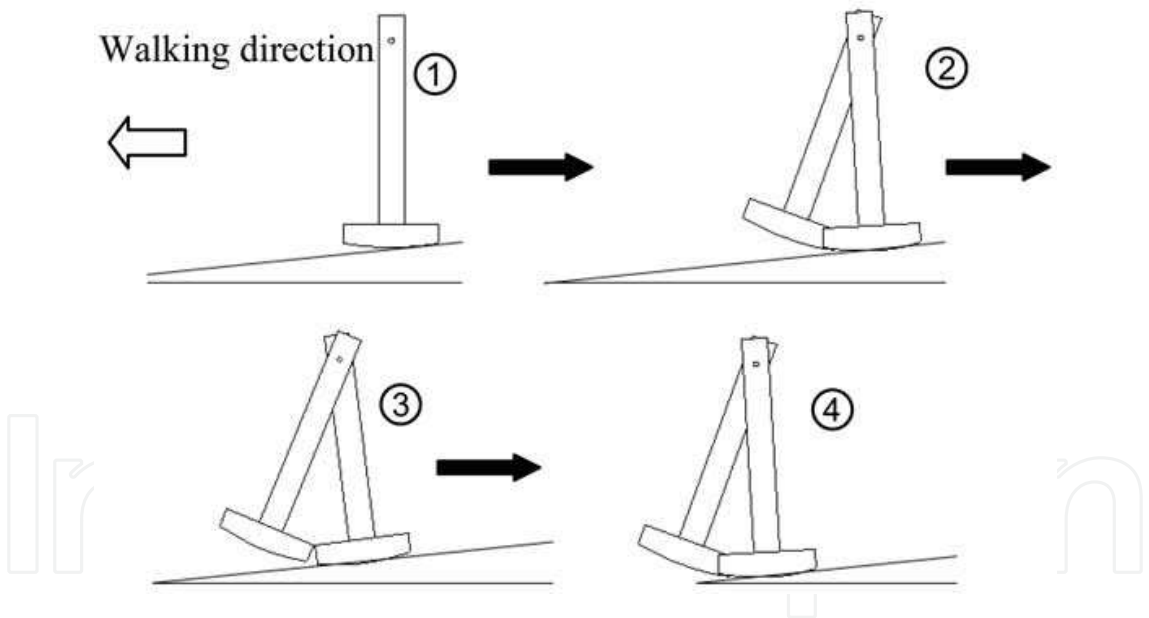

Fig. 6. One cycle of gait for Sagittal Plane Mode

Fig. 7 shows the angle of legs toward waking direction from the beginning of walking for 5 seconds. It seems it will take some time for stable walking. The vertical dotted line in Fig. 7 shows the moment for changing the support leg. The period between changing legs hardly changes even after 30 seconds has passed.

Fig. 8 shows the phase plane locus for angle of legs. The trajectory starts from the initial condition, $(k_{ns}, k_s, \dot{k}_{ns}, \dot{k}_s) = (0,0,0,0)$ shown as scene 1 in Fig. 6, and converges into the same trajectory (the limit cycle) after 7 cycles of gait.
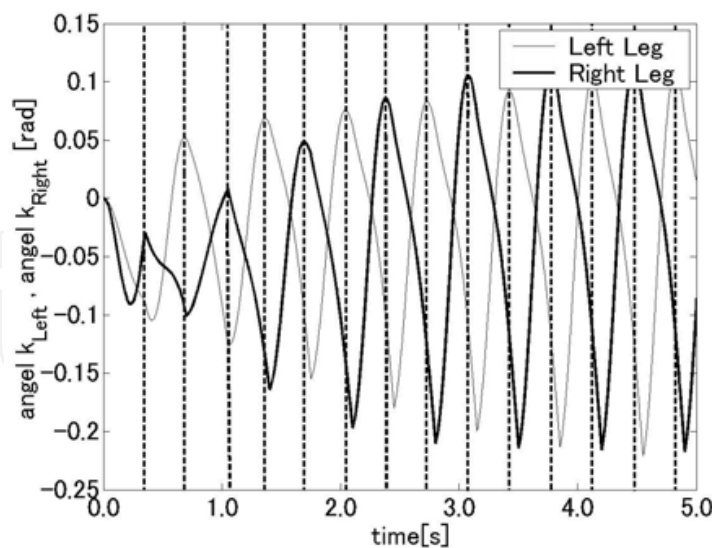
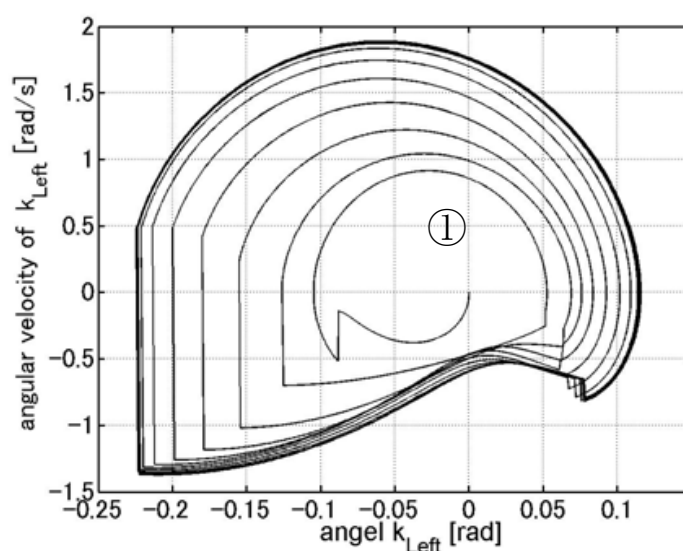Fig. 7. Leg Angle in Sagittal Plane

Fig. 8. Phase Plane Locus in Sagittal Plane

3.3 Effects of initial conditions and structural parameters

It is likely that initial conditions and structural parameters are the important factors for stable walking. So, some simulations are performed in this manner.

The limit cycles can be observed under these conditions by changing angle of slope from 0.017 to 0.087 rad shown in Fig. 9. By looking some data from leg angle, the walker is able to walk down the slope. However, some differences are observed in the trajectory of limit cycle as Fig. 9. Places circled are the position where the swing leg is changing to support leg. The length of the vertical line seems to have some effect on the stability of walking. The better condition for stable walking was (c) in Fig. 9. The angle of swing leg to contact the surface of slope seems to be important parameter.

In addition, the effects of structural parameters can be observed in Fig. 10. The ratio of inertia to mass has been changed in order to see phase locus plane. The ratio of stable

walking shown above is 38 to 1 in Fig. 10 (a), and all the other conditions are from Table 1 and 2. When ratio decreases to 37 to one, it showed very similar limit cycle. However, the limit cycle starts to change its shape for less stable walking as ratio decreases. When ratio increases, limit cycle is not observed any longer as shown in Fig. 10 (b).

It is also true that the limit cycle is the same as long as the ratio of inertia to mass does not change under same initial conditions. In another word, when the mass and inertia are changed to half without changing the ratio of inertia to mass, the limit cycle is the same as the initial mass and inertia.
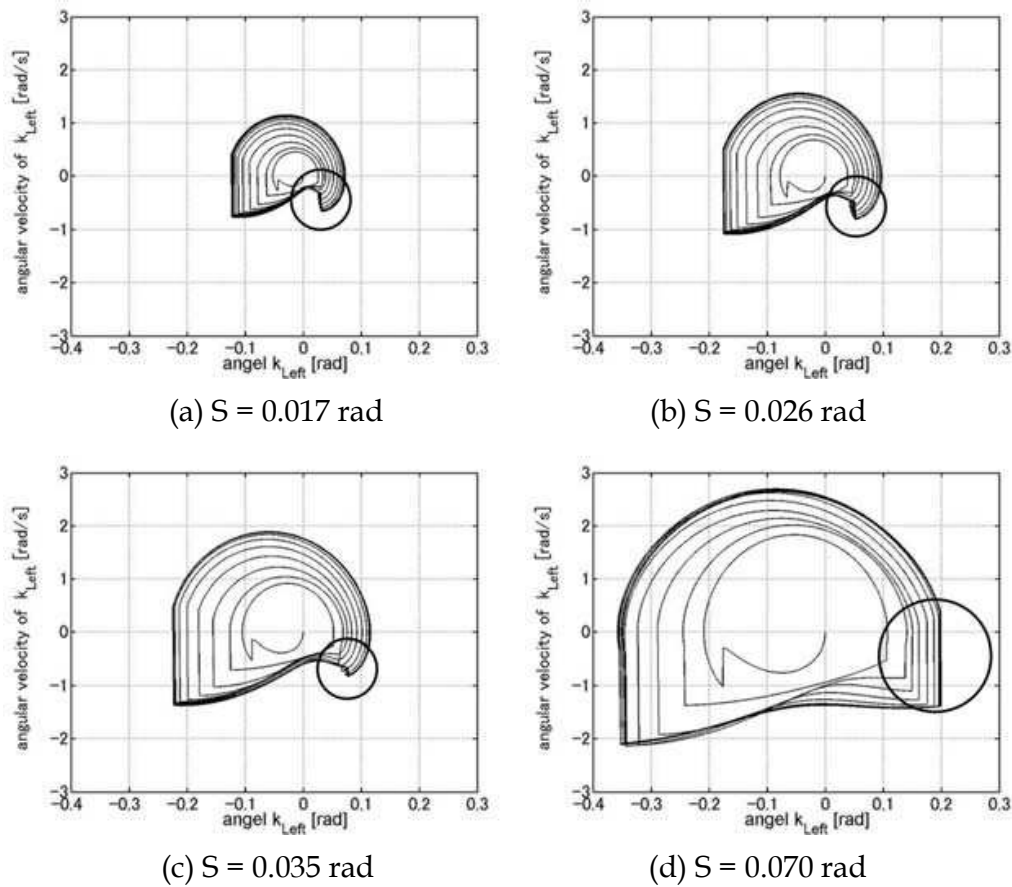

(a) S = 0.017 rad   (b) S = 0.026 rad

(c) S = 0.035 rad   (d) S = 0.070 rad

Fig. 9. Phase Plane Locus by Changing Angle of Slope
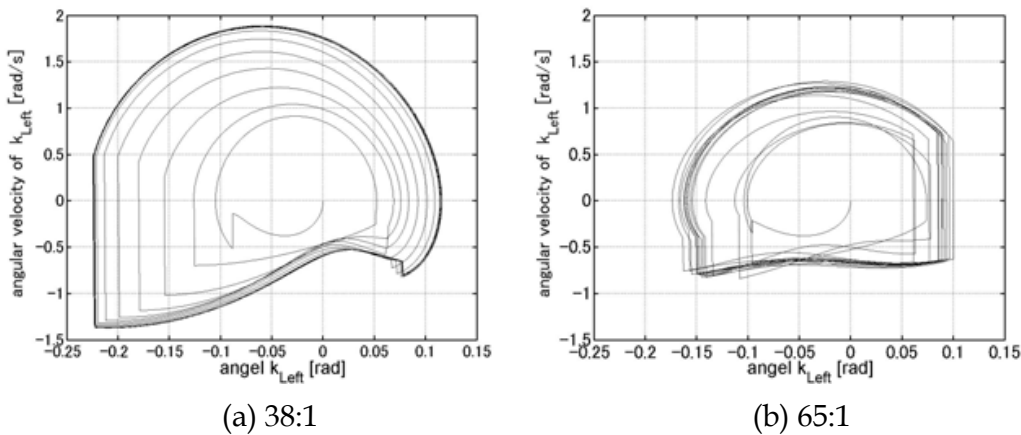

(a) 38:1   (b) 65:1

Fig. 10. Change in Phase Locus Plane by Changing Ratio of Inertia to Mass (Inertia: Mass)

4. Experimental analyses

For experimental analyses, 3D bipedal passive dynamic walker was build upon the structural parameters from simulation analyses. Experiments were performed around the conditions obtained from the simulation analyses for the walker.

4.1 3D passive walker and experimental method
3D passive walker in this study has two straight legs and two curved foot. The feet have 3D concave up surface with a curvature in each plane, such as 500mm in lateral plane, and 380 mm in Sagittal plane.

A picture of 3D passive walker is shown in Fig. 11. Table 1 and 2 show the other parameters of the walker.

This walker (Fig. 11) has no actuators, and has two legs those are connected together at hip with simple link structure. It is designed after the waking model from Fig. 1. A three dimensional sensor (VC-03, Sensation Inc.) is used. The sensor set on the left hip, as shown in a circle of Fig.11, in order to measure the angle of leg and rolling angle at walk. This sensor can be connected to the computer for real time reading of the angle.

Experiments were performed with 3D passive walker under conditions from the simulation. The initial conditions are used from Table 1 and 2. The angle of slope is set to be 0.035 rad, and $(u, \ddot{u}) = (0.18,0)$ for walking. Some of the initial conditions and structural parameters are varied to see the change in walking. Also, the surface of slope for walking was covered with a rubber sheet for inelastic collision between foot and slope. The rubber sheet may allow the walker decrease yaw motion.
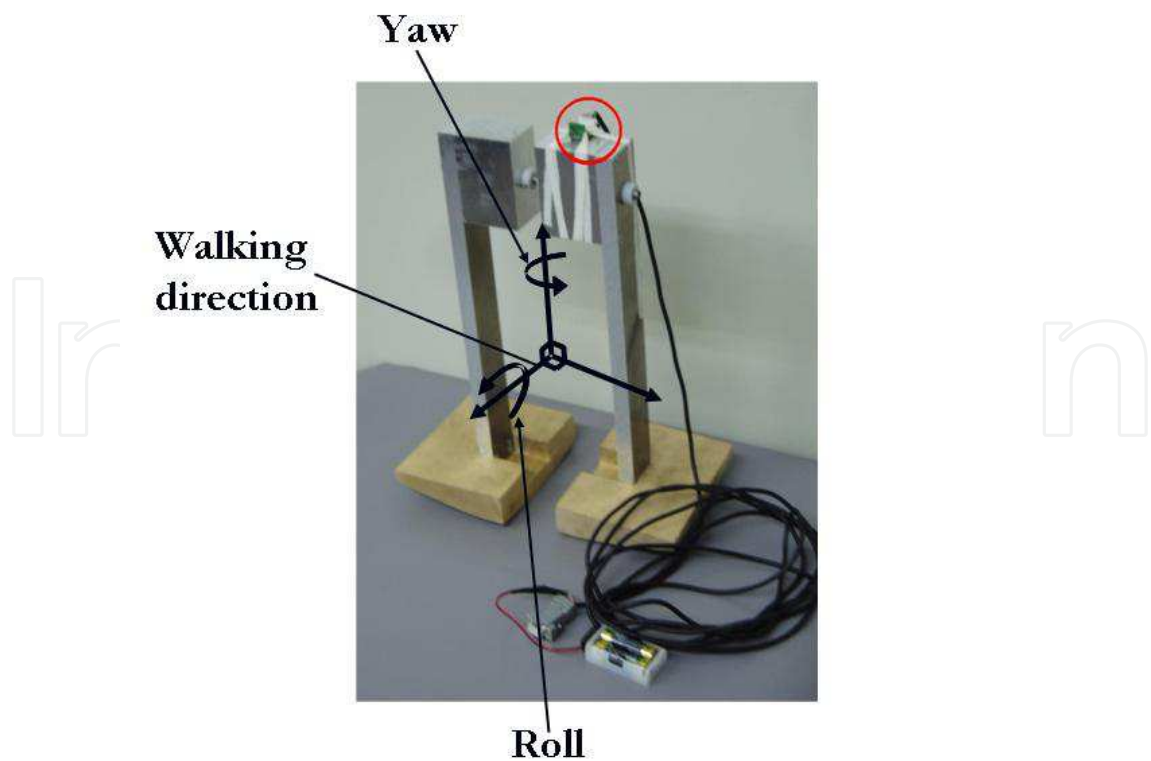

Fig. 11. 3D Passive Walker

Toward Human Like Walking – Walking Mechanism of 3D Passive
Dynamic Motion with Lateral Rolling– Advances in Human-Robot Interaction

201

4.2 Results

The change in angle of roll is shown in Fig. 12. Although the initial condition is $(u, \ddot{u}) = (0.18, 0)$, the rolling angle shows larger amplitude.

Fig.13 shows the change in angle of left leg with time. Each axis shows time and angle of left leg, horizontal and vertical. This shows the walking motion from the beginning to 6 seconds. However, the yaw motion becomes greater after 6 seconds so that it is hard to measure the angle of left leg correctly.

In addition, the angle of slope is changed from 0.017 to 0.070 rad in order to see effect for walking. The walker is able to walk down the slope for under those angles. However, the gait for waking is different. When the angle is 0.087 rad, the walker can walk down the slop, but falls down from time to time. The better angle for stable walk is around 0.035 rad.

Although the further study is necessary, the changes for other parameters, such as adding weight on foot, cause the change in gait.
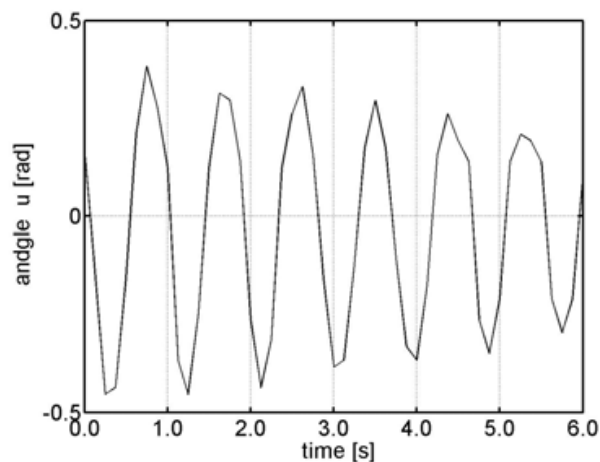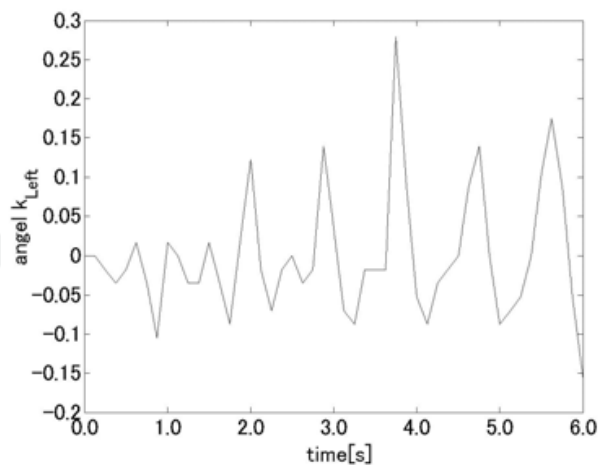

Fig. 12. Change in Angle of Roll

Fig. 13. Change in Angle of Leg

4.3 Discussion

Under one of the best initial conditions (including the structural parameters) for the stable walking, the 3D passive walker showed stable walking. This matching condition is meaningful for further investigation. At the beginning of the walking, the walker shows

very little yaw motion. However, the walker started to show yaw motion greater than expected. The rubber sheet was not enough to compensate the yaw motion.

So, further study is necessary to decrease effects of yaw motion. During human walk, left arm is swung as right leg is stepped forward and right arm is swung as left leg is stepped forward. Arms are attached around hip of 3D passive walker to compensate the yaw motion by swinging arms by imitating human walking.

The other way to decrease yaw motion is also planned as a next study. The leaf spring is made like a body of dinosaur or lizard in order to compensate the yaw motion by spring force and inertia.

Both studies are just started. The further investigations are necessary to be reported.

5. Discussion

Fig.14 shows the comparison of angle of left leg between simulation and experiment according to time in sagittal plane. The vertical axis is for leg angle, and horizontal axis is for time. The solid line is for a result of simulation, and dotted line is for a result of experiment. Both simulation and experiment are continued for 6 seconds.

The initial condition for Fig.14 was derived from the simulation analysis. This condition was one of the best for stable walking. Both results have similar tendency qualitatively. But experimental results seem to have time lag to the simulation result.
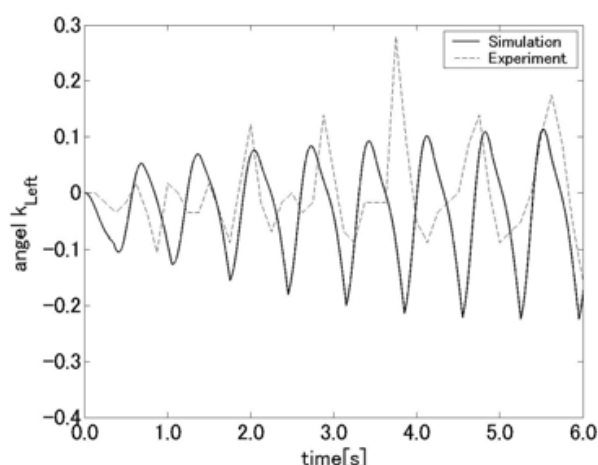

Fig. 14. Angle of Leg by Simulation and Experiment

There are reasons for this time lag to be happened, such as a friction around linkage around hip, friction between foot and surface of floor, and so on. One of the main reasons is from the yaw motion. Because of the yaw motion, the angle of leg cannot be measured correctly for this experiment.

In addition, the change in angle of slope showed similar tendency between simulation and experiment. Especially when the angle of slope is around 0.070 rad, the walker was able to walk down the slope but falls on back very often in experiment. Fig. 9 (d) shows the swing leg becomes to support leg at the point where the swing leg does not become zero angular velocity. This can be read as the reason for the walker fall on back from experiments.

Fig.15 shows change in angle of roll from simulation and experiments. The amplitude is larger for the experiments and the attenuation is much greater in the experiments. The attenuation is probably caused by the rubber sheet, collision to the slope and yaw motion.

The reason for larger amplitude seems to be relating with initial condition for walking experiments.

So, additional analysis was performed in simulation, because the initial condition can be created easily. The initial angular velocity is changed for simulation from 0 to –2.1 rad/s. Fig. 16 shows similar tendency for angle of roll in the beginning. The amplitude of roll becomes similar although attenuation is larger in experiment as before. This gives some attention the initial conditions should be considered carefully especially in experiments.
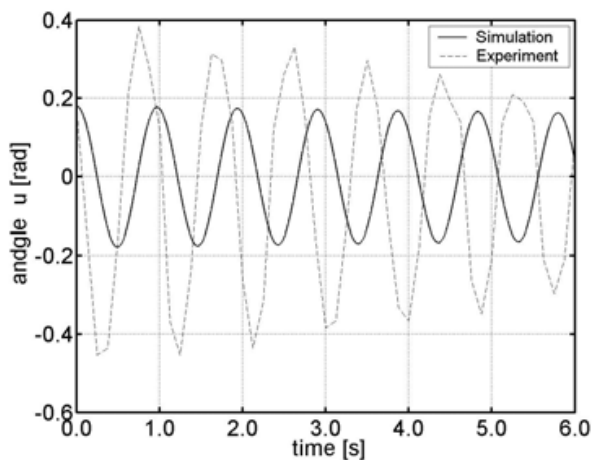
Fig. 15. Angle of Roll by Simulation and Experiment
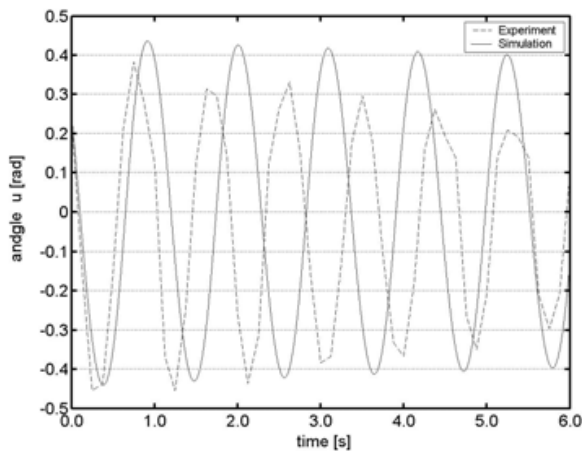
Fig. 16. Angle of Roll by Simulation with Initial Angler Velocity (-2.1rad/sec)

6. Conclusion

As the fist step for the advance in human-robot interaction, it is important to determine the stability of 3D walking model, and to find initial conditions and structural parameters for stable walking as a first step.

The simulation was performed to search of structural parameter for stable walking condition. A 3D walker is build according to the simulation result. Then, the experimental analysis was carried out to search some parameters and compare with simulation result.

Simulation shows some parameters and initial condition would lead stable walking for 3D model in Table 1 and 2. The experimental analysis shows 3D passive walker walks down the

slope under the same condition from simulation result, and angle of legs has similar tendencies as to the simulation results. Although the tendency from the experiments and simulations are similar, the results show some differences such as time lag for leg angle in sagittal plane. One of the main reasons for this seemed to be caused by assumption that the yaw motion is small enough to ignore. So, further trials to decrease or separate the effects from yaw motion would lead better simulation for stable walking and better understanding of passive walking. And more over, the humanoid robot may be able to walk more efficiently. These studies will help interaction between human and robot.

7. References

A. Ishiguro, D. Owaki, "Toward a Well-balanced Control," ISCIE, vol. 49, no. 10, 2005, 417-422. ISSN   0916-1600

K. Osuka, "Legged Robots and Control Scheme based on a Sence of Passive Dynamic Walking," RSJ Journal, vol.20, no.3, 2002, 233-236. ISSN   0289-1824

T. McGeer, "Passive Dynamic Walking," Int. J. of Robotics Research, vol.9, no.2, April, 1990, 62-82. ISSN   0278-3649

A. Goswami, B. Thuilot and B. Espiau, "Compass-Like Biped Robot-Part I: Stability and Bifurcation of Passive Gaits," Technical Report 2996, INRIA, 1998.

A. Goswami, B. Thuilot and B. Espiau, "A Study of the Passive Gait of a Compass-Like Biped Robot: Symmetry and Chaos," The Int. J. of Robotics Research, vol.17, no.12, 1998, 1282-1301. ISSN   0278-3649

K. Osuka, T.Fujitani and T.Ono, "Passive Walking Robot QUARTET," Proc. of the 1999 IEEE Int. conf. on Control Application, 1999, 478-483. ISBN 0-7803-5446-X

K. Osuka and K. Kirihara, "Motion Analysis and Experiment of Passive Walking Robot Quartet II," RSJ Journal, vol.18, no.5, 2000, 737-742. ISSN   0289-1824

R. Tedrake, "Applied Optimal Control for Dynamically Stable Legged Locomotion," PhD thesis, MIT, 2004.

R. Tedrake, T. W. Zhang, M. F. Fong, and H. S. Seung, "Actuating a Simple 3D Passive Dynamic Walking," ICRA, vol.5, April, 2004, 4656-4661. ISBN 0-7803-8232-3
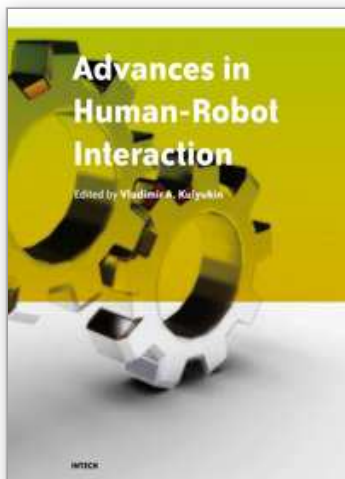
Advances in Human-Robot Interaction

Edited by Vladimir A. Kulyukin

Rapid advances in the field of robotics have made it possible to use robots not just in industrial automation but also in entertainment, rehabilitation, and home service. Since robots will likely affect many aspects of human existence, fundamental questions of human-robot interaction must be formulated and, if at all possible, resolved. Some of these questions are addressed in this collection of papers by leading HRI researchers.

How to reference

In order to correctly reference this scholarly work, feel free to copy and paste the following:

Tomoo Takeguchi, Minako Ohashi and Jaeho Kim (2009). Toward Human Like Walking – Walking Mechanism of 3D Passive Dynamic Motion with Lateral Rolling – Advances in Human-Robot Interaction, Advances in Human-Robot Interaction, Vladimir A. Kulyukin (Ed.), ISBN: 978-953-307-020-9, InTech, Available from: http://www.intechopen.com/books/advances-in-human-robot-interaction/toward-human-like-walking-walking-mechanism-of-3d-passive-dynamic-motion-with-lateral-rolling-advanc

INTECH
open science | open minds